Article

J. Mex. Chem. Soc. **2025**, *69*(4)
Regular Issue

ISSN-e 2594-0317

Impact of the Chemical Speciation of the Ag^+–Cl^-–e^- System on the Construction of True Reference Electrodes and the Potential Purification of the Ionic Liquid 1-Butyl-3-Methylimidazolium Bis(Trifluoromethylsulfonyl)Imide

Jorge Ruvalcaba-Juárez, Oscar Valenzuela-Bonilla, Norma Rodríguez-Laguna, Arturo García-Mendoza*

Sección de Química Analítica, FES Cuautitlán, Universidad Nacional Autónoma de México, Av. Primero de Mayo S/N, Estado de México, 54740, México.

***Corresponding author:** Arturo García-Mendoza, email: arturogm@unam.mx

Received October 9th, 2024; Accepted February 11th, 2025.

DOI: http://dx.doi.org/10.29356/jmcs.v69i4.2374

Abstract. We present the chemical speciation of $[AgCl_n]^{1-n}/Ag^0$ redox couple in two media: the room temperature ionic liquid (RTIL) 1-butyl-3-methylimidazolium bis(trifluoromethylsulfonyl)imide ($[C_4mim][NTf_2]$) as a model ionic solvent, and aqueous medium. The logarithms of the formation constants ($\log \beta_n$), solubility product constant (pK_{sp}), and formal reduction potential (E°') values of these chemical systems were estimated through open circuit potential measurements using suitable indicator electrodes and representative potentiometric titrations. The estimation of the extraction constant (K_E) of Ag^+ in the interphase water-RTIL was determined through a series of extraction systems at different values of $p(V_{org}/V_{ac})$, finding that the extraction of silver(I) is favorable towards aqueous media at high pCl values. Also, a series of reference electrodes (RE) were constructed under different buffer conditions for use in this ionic liquid to assess the utility of the collected electrochemical data. The potential drift of the half-cells was determined via cyclic voltammetry using the cobaltocene redox couple, $[Co(Cp)_2]^{+/0}$, as an internal redox reference; in addition, information on the Ag(I) extraction constant allowed to explain the effect of water as a contaminant of these devices. Finally, specific configurations were identified for these REs, some exhibiting potential drifts of less than 0.58 $\mu V\ h^{-1}$, rendering them comparable to commonly used REs in aqueous media.
Keywords: Room temperature ionic liquids; reference electrodes; silver; chemical speciation; liquid-liquid extraction.

Resumen. Se presenta la especiación química del par redox $[AgCl_n]^{1-n}/Ag^0$ en dos medios: el líquido iónico a temperatura ambiente (RTIL) bis(trifluorometilsulfonil)imida de 1-butil-3-metilimidazolio ($[C_4mim][NTf_2]$) como solvente iónico modelo, y en medio acuoso. Los logaritmos de las constantes de formación ($\log \beta_n$), la constante del producto de solubilidad (pK_{ps}) y los valores del potencial formal de reducción (E°') de estos sistemas químicos se estimaron mediante mediciones de potencial de circuito abierto utilizando electrodos indicadores adecuados y valoraciones potenciométricas representativas. La estimación de la constante de extracción (K_E) de Ag^+ en la interfase agua-RTIL se determinó a través de una serie de sistemas de extracción a diferentes valores de $p(V_{org}/V_{ac})$, encontrando que la extracción de plata(I) es favorable hacia el medio acuoso a altos valores de pCl. Además, se construyó una serie de electrodos de referencia (RE) bajo diferentes condiciones de amortiguamiento para su uso en este líquido iónico, con el fin de evaluar la utilidad de los datos electroquímicos obtenidos. La deriva potencial de las semiceldas se determinó mediante voltamperometría cíclica usando el par redox de cobaltoceno, $[Co(Cp)_2]^{+/0}$, como referencia redox interna además, la información sobre la constante de extracción de Ag(I) permitió explicar el efecto del agua como contaminante de estos dispositivos. Finalmente, se identificaron configuraciones específicas para estos

J. Mex. Chem. Soc. **2025**, *69*(4)
Regular Issue

ISSN-e 2594-0317

REs, algunos de los cuales exhibieron derivas potenciales de menos de 0.58 μV h^{-1}, haciéndolos comparables con los REs comúnmente utilizados en medios acuosos.
Palabras clave: Líquidos iónicos a temperatura ambiente; electrodos de referencia; plata; especiación química; extracción líquido-líquido.

Introduction

Room-temperature ionic liquids (RTILs) are liquid ionic salts at temperatures below 100 °C [1]. These primarily consist of a bulky organic cation with heteroaromatic atoms and an inorganic anion with low coordinating capacities [2–4]. Given the vast cation-anion combinations and their functionalization capacity, many of these compounds have been documented, each offering versatility and multiple applications in various areas of chemistry. Ionic liquids are used as solvents and supporting electrolytes in routine electrochemical analysis due to their board electroactive window and high specific conductivity, enhancing measurement sensitivity and reproducibility. They are applied in electrochemical sensors for selective detection of redox species, in cyclic voltammetry to study electrochemical stability and electron transfer kinetics, and in controlled electrodeposition systems for characterizing metal film growth processes [5–7].

The reagents used for the synthesis of ionic liquids (ILs) often involve the presence of several metal cations, such as silver, involved in metathesis reactions [8], resulting in solvents that are not entirely pure. Thus, their use as solvents to increase reaction rates and enhance efficiency is a function of their initial purity [9]; furthermore, it must be considered that such processes generate contaminated ionic liquids as waste. Although significant interest in ILs for various applications stems from their properties as solvents, these acquire reference values under certain purity conditions, so achieving successful, sustainable, and economical purification remains a significant challenge.

Reference electrodes (REs) are compartmentalized devices that maintain a known and constant half-cell potential over time due to the presence of a redox couple in a buffered condition. However, the absence or alteration of the relative concentrations of the chemical species defining the specific redox couple will inevitably affect the observed electrode potential [10,11] . In Room Temperature Ionic Liquids (RTILs), several studies have focused on developing reference electrodes, such as Snook *et al*., who proposed a Ag^0/Ag^+ electrode, but interactions with the RTIL's ions can compromise its stability and accuracy [12] . Huber and Roling developed a micro Ag^0/Ag^+ reference electrode, useful for small systems, though its long-term performance in RTILs remains unvalidated [13] . Horwood and Stadermann introduced a $Ag^0/Ag_2S_{(s)}$ electrode with greater stability, but its use is limited to certain RTILs [14]. García-Mendoza and Aguilar-Cordero designed a $Ag^0/[AgCl_n]^{1-n}$ electrode for bis(trifluoromethylsulfonyl)imide-based RTILs. However, its application is not generalizable to other ionic liquids composed of different types of anions [15].

These electrodes must be specifically designed for the solvent in which they are used to ensure stability and accuracy. Properly designed electrodes offer several advantages: (1) reproducible and stable potential over time, (2) reversibility and adherence to the Nernst equation, (3) return to the initial value after a small current is applied and the stopped, and (4) no hysteresis with temperature cycling [16–18] . Thus, it is essential to construct reference electrodes tailored explicitly to the RTIL being studied to ensure reliable and analytically acceptable measurements.

Unfortunately, quasireference electrodes (QREs) are often used when nonaqueous solvents are used. These devices maintain a potential value, albeit not well-defined or reproducible, during a series of measurements [19]. This kind of electrode must be calibrated with respect to an internal reference system to obtain meaningful potential values. Commonly used redox couples for this purpose include ferrocenium/ferrocene ($[Fe(Cp)_2]^{+/0}$) and cobaltocenium/cobaltocene ($[Co(Cp)_2]^{+/0}$) [20]. Furthermore, in QREs, the redox couple responsible for the electrode potential is uncertain, as multiple uncontrolled processes can occur at the metal-solution interface [21,22]. Furthermore, the destruction of QREs in RTILs due to their solubilization effect has been reported [2], making their use not recommended for electrochemical assays conducted over extended periods or for the characterization of processes occurring in the electric double layer (EDL) [23,24].

This work aims to describe the chemical speciation of the Ag^+–Cl^-–e^- system in $[C_4mim][NTf_2]$ and the extraction of Ag(I) from this RITL towards water, using a variety of electrochemical techniques to analyze the chemical species involved in potential drift in different architectures of true reference electrodes of Type 1 and Type 2 based on the concurrent interfaces $Ag^0|Ag^+||$ and $Ag^0|AgCl_{(s)}||$, respectively. The goal is to propose

J. Mex. Chem. Soc. **2025**, *69*(4)
Regular Issue

ISSN-e 2594-0317

these half-cells as constant potential electrodes for use in $[C_4mim][NTf_2]$, thereby minimizing the need for toxic materials, such as mercury, and expensive ones, like platinum or palladium [22,25,26]. Additionally, estimating the silver extraction constant at the water-RTIL interface is intended to provide comments on the exposure of prepared REs in humid environments. This information could be used as a competitive, environmentally friendly, and cost-effective purification technique, as it reduces the use of toxic, volatile, and flammable contaminants required in other methods, such as distillation. Estimating this extraction constant allows us to understand the partitioning behavior of silver(I) between the two phases, considering the effect of their pCl imposed values, pH in the aqueous phase, and the volume ratio of the solvents, $p(V_{org}/V_{ac})$.

Experimental methodology

Reagents

The aprotic ionic liquid used in this work was 1-butyl-3-methylimidazolium bis(trifluoromethylsulfonyl)imide ($[C_4mim][NTf_2]$, Merck, purity ≥ 98 %). For the chemical speciation of the $AgCl_{(s)}/[AgCl_n]^{1-n}$ and $Ag^{+/0}$ systems, silver wire (Ag^0, Sigma–Aldrich, diameter = 1.0 mm, purity ≥ 99.99 %), 1-ethyl-3-methylimidazolium chloride ($[C_2mim]Cl$, Sigma–Aldrich, purity > 98 %), and silver bis(trifluoromethylsulfonyl)imide ($Ag[NTf_2]$, Sigma–Aldrich, purity > 97 %) were used. These materials were common for the construction of the RE in the RTIL. For the identification of the intrinsic solubility of silver in the RTIL, a medium composed of silver nitrate ($AgNO_3$, Sigma–Aldrich, purity ≥ 99.0 %), potassium thiocyanate (KSCN, Sigma–Aldrich, purity > 98.5 %), ammonium nitrate (NH_4NO_3, Sigma–Aldrich, purity ≥ 98 %), sodium sulfite (Na_2SO_3, J.T. Baker, purity ≥ 98.52 %), and sodium thiosulfate pentahydrate ($Na_2S_2O_3 \cdot 5H_2O$, J.T. Baker, purity ≥ 99.5 %) was used. Cobaltocenium hexafluorophosphate ($[Co(Cp)_2][PF_6]$, Sigma–Aldrich, purity ≥ 98 %) was used as an internal reference system in the RTIL, while ferrocenemethanol ($[Fe(Cp)_2CH_2OH]$), Sigma–Aldrich, purity ≥ 97 %) was used as a redox standard in aqueous solution. The reagents were used as received and stored in a desiccator cabinet Bel-Art Amber tinted UV blocking model (relative humidity < 5 %). The $[C_4mim][NTf_2]$ and all solutions prepared in this RTIL as a solvent were dried for 24 h at 90 °C in an oven before use. Deionized water (> 18 MΩ cm^{-1}) obtained from a Milli-Q system was used for washing. Nitrogen 4.8 (N_2, ProSpec, purity ≥ 99.998 %) was used to perform measurements under an inert atmosphere using an appropriate gas−washing glass bottle.

Instruments

For open circuit potential (OCP) measurements and the electrochemical preparation of $AgCl_{(s)}$ coatings, a potentiostat (model 920C, CH Instruments, USA) with a three-electrode setup was used. A silver wire (Ag, Sigma–Aldrich, purity ≥ 99.99 %, 1.0 mm diameter, 30 mm length) was used as the working electrode (WE), a platinum coiled wire (Pt, Sigma–Aldrich, purity ≥ 99.99 %, 0.5 mm diameter, 37 mm length) was used as the counter electrode (CE), and an appropriate RE was utilized. For electrochemical measurements by cyclic voltammetry (CV), a potentiostat (PalmSens4 model, Palm Sens BV, NL) with a three-electrode setup was used. A gold electrode (Au, CH Instruments, 2.0 mm diameter) and a glassy carbon electrode (GC, CH Instruments, 3.0 mm diameter) were employed as working electrodes (WEs); a platinum coiled wire described above was the counter electrode (CE). A Faraday cage (Cypress Systems, USA) was utilized to minimize electrostatic interferences during data acquisition.

Every working electrode was polished with alumina powder (Buehler) with a particle size of 0.05 μm on a microcloth (Buehler) and washed with deionized water (> 18 MΩ cm^{-1}). Immediately, electrodes were sonicated in an appropriate volume of this solvent for 5 min and finally rinsed. Afterward, the electrodes were placed under a flow of dry N_2. All masses were measured using a Mettler balance (XP105DR, ± 0.01 mg, Mettler Toledo, USA). Gravimetric and volumetric errors were typically less than 2 %.

The temperature was ensured at T = 25.0 ± 0.5 °C using a recirculating water bath connected to an optimized thermostated electrochemical cell. The arrangement of the three-electrode cell used is shown schematically in Fig. 1.

J. Mex. Chem. Soc. **2025**, *69*(4)
Regular Issue

ISSN-e 2594-0317

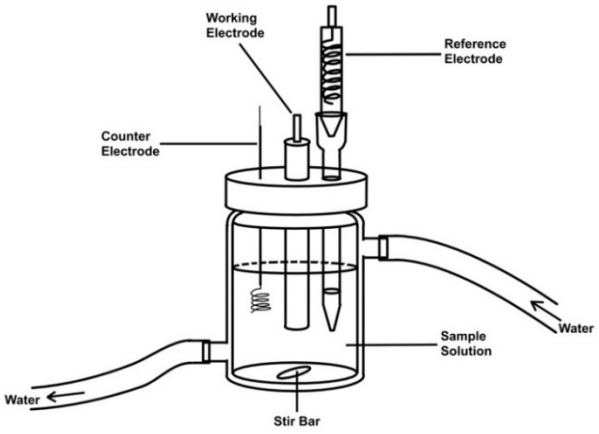

Fig. 1. Schematic of the three-electrode cell setup for electrochemical measurements using a thermostated cell.

Electrochemical measurements

All electrochemical measurements were conducted under a dry N_2 atmosphere by bubbling the gas into a cell with a maximum solution volume of 2.0 mL. The evolution of the RE potential values over time was determined *vs.* the cobaltocene/cobaltocenium redox couple ($[Co(Cp)_2]^{+/0}$) using CV at nine scan rates in V s^{-1}: 0.005, 0.010, 0.025, 0.050, 0.100, 0.250, 0.500, 0.750, and 1.000. The redox standard solution was prepared by weighing the necessary amount of cobaltocenium hexafluorophosphate in $[C_4mim][NTf_2]$ and stirring under a stream of dry N_2 until complete dissolution of the solid. Care was taken to ensure that the concentration was the same in all solutions of the redox standard ($C \approx 25$ mmol L^{-1}), achieving a similar final total mass for all the solutions used by weighing the same amount of ionic liquid and standard. During data acquisition, compensation was made for up to 95% of the electrical resistance of each solution in the form of an ohmic drop, iR.

The OCP of the $[C_2mim]Cl$ and $Ag[NTf_2]$ solutions prepared in the RTIL was monitored in triplicate for 600 s at intervals of 0.2 s using Ag^0 and $AgCl_{(s)}$ wires as convenient indicator electrodes, a Pt wire as the CE, and a freshly calibrated RE with respect to the $[Co(Cp)_2]^{+/0}$ redox couple. In aqueous media, the OCP of the NaCl solutions prepared in water was monitored for 600 s at intervals of 0.2 s using a $AgCl_{(s)}$ wire, a Pt wire as the CE, and a freshly calibrated RE with respect to the $[FcMeOH]^{+/0}$ redox couple.

The determination of Ag(I) in the aqueous phase was carried out through potentiometric titrations because the estimated concentration falls within the technique's linear limit of quantification. Potentiometric monitoring was performed with a three-electrode system using a silver wire as the indicator electrode (IE), a platinum wire as CE, and a $Ag^0/AgCl_{(s)}$ RE. A salt liquid junction containing a saturated KNO_3 solution was used to prevent the migration of Cl^- ions from the internal electrode chamber into the solution. The OCP was measured for 300.0 s with stirring. Aliquots of 10.0 µL of a 0.1 M sodium chloride standard solution were added to the aqueous solution, and the OCP was measured after each addition.

The determination of Ag(I) in the nonaqueous phase, $[C_4mim][NTf_2]$, was carried out using Anodic Stripping Square Wave Voltammetry (ASSWV) because the estimated concentration range falls within the technique's linear limit of quantification. This analysis was performed using a glassy carbon electrode as WE in a coordinating medium prepared in an aqueous solution in which a calibration curve was constructed using standard additions of a previously standardized $AgNO_3$ solution.

Preparation of extraction systems

Two experimental setups were devised to evaluate the silver extraction constant. The pH of the aqueous phase was buffered using a Britton-Robinson buffer solution, which was prepared to achieve the desired pH for the study.

For the first setup, an average volume of 0.4 mL of pure $[C_4mim][NTf_2]$ was weighed into a glass vial, followed by the addition of an average volume of 0.6 mL of a silver nitrate solution (0.095 ± 0.001 M) using a micropipette. The mixture was stirred for 15 min and left to rest for 24 h in the dark before phase separation.

J. Mex. Chem. Soc. **2025**, *69*(4)
Regular Issue

ISSN-e 2594-0317

For the second setup, an average volume of 0.4 mL of a previously prepared solution of silver bis(trifluoromethylsulfonyl)imide in $[C_4mim][NTf_2]$ was measured. Then, an average volume of 0.6 mL of deionized water or Britton-Robinson buffer solution was added to the sample in the glass vial. The mixture was stirred for 15 min and stored in the dark for 24 h before phase separation.

The independent phases were preserved in glass vials for subsequent quantification.

Construction of reference electrodes

Four REs were fabricated. Two were based on the $Ag^0|AgCl_{(s)}|Cl^-||$ half-cell, one based on the $Ag^0|Ag^+||$ half-cell, and another on $Ag^0|Cl^-||$ half-cell. A detailed description of the construction and labeling of the REs is provided in Appendix A, Supporting Information.

Results and discussion

Potentiometric calibration curves

The $Ag^0|AgCl_{(s)}$ interface coating was produced through CV using an acidic medium in an aqueous solution. Due to the imposed pCl value in the solution, there is no predominant presence of $[AgCl_n]^{1-n}$ type complexes, with $1 \leq n \leq 4$ [27]. All coatings were visually inspected and presented a white color without cracks or dark spots. They were dried under N_2 flow and stored in the dark for two days before being used in the RTIL.

A relationship was observed between the OCP values obtained when using Ag^0 and $Ag^0|AgCl_{(s)}$ working electrodes and the logarithm of the concentration of chloride and silver(I) solutions prepared in $[C_4mim][NTf_2]$. This behavior fits linear relationships according to the archetypal model of the Nernst-Peters equation [18], where the slope corresponds to the number of particles exchanged at equilibrium responsible for the potential at the interface in terms of multiples of the quotient 2.3RT/F, as illustrated in Fig. S2 (Appendix B, Supporting Information). Thus, when using a Ag^0 indicator electrode, a reversible and linear response is obtained over the entire range of analyzed concentrations of $Ag[NTf_2]$ in the RTIL, as shown in the first row of Table S2, suggesting a Nernst equation that coincides with the linear fit of E *vs*. log (C/M), where the intercept of the linear fit yields the value of E°'/V for the $Ag^{+/0}$ redox couple. Furthermore, when using a $Ag^0|AgCl_{(s)}$ indicator electrode for these same solutions, a similar OCP response is obtained, expressed in terms of a Nernst equation, as indicated in the second row of Table S2. The intercept obtained from the linear fit is linked to the K_{sp} value of the $AgCl_{(s)}/Ag^+$ couple.

On the other hand, when a $Ag^0|AgCl_{(s)}$ or Ag^0 indicator electrode is used to measure the potential of $[C_2mim]Cl$ solutions of different concentrations prepared in the ionic liquid, the same OCP response is obtained regardless of the WE used. There is experimental evidence of the solubilization of $AgCl_{(s)}$ due to excess Cl^- in molecular solvents and in other RTILs that share structural similarities and physicochemical properties with $[C_4mim][NTf_2]$ [28]. Hence, the formation of $[AgCl_n]^{1-n}$ chemical species in this ionic medium, potentially responsible for the electrode potential at the interface, is probable. Thus, the chemical equilibrium presented in the third and fourth rows of Table 2S is presumed to be responsible for the electrode potential due to the presence of the stabilized $[AgCl_3]^{2-}$ species [15]. These data are accompanied by a Nernst equation, whose intercept the E°'/V of the $[AgCl_3]^{2-}/Ag^0$ redox couple can be estimated.

The potentiometric methodology presented was replicated in an aqueous medium (Fig. S3) to calibrate the $Ag^0/AgCl_{(s)}$ electrode for potentiometric titrations in this medium. Additionally, this methodology allows for determining the number of particles exchanged in the redox pair. According to the experimental results, a slope corresponding to a single particle exchanged in both equilibria was obtained, consistent with what has been reported in the literature (Table S2) [29].

An alternative study to corroborate the number of electrons exchanged in the redox system of the Ag^0/Ag^+ pair in $[C_4mim][NTf_2]$, similar to what occurs in aqueous medium, was performed through chronopotentiometric studies in both aqueous medium and the ionic solvent. The results confirmed the exchange of a single particle (Appendix D, Supporting Information).

Potentiometric titrations

A series of representative potentiometric titrations were carried out in both $[C_4mim][NTf_2]$ and water to obtain information related to the characteristic chemical equilibria of each stage of the analytical process, to elucidate the chemical speciation of the Ag^+–Cl^- system [15]. The general scenarios are established as follows.

J. Mex. Chem. Soc. **2025**, *69*(4)
Regular Issue

ISSN-e 2594-0317

In the first scenario, the potentiometric titration of a $[C_2mim]Cl$ solution was performed, to which aliquots of $Ag[NTf_2]$ as the titrant were added, both solutions prepared in $[C_4mim][NTf_2]$. Potentiometric monitoring was performed using a $Ag^0|AgCl_{(s)}$ as an indicator electrode, previously calibrated with a series of Cl^- solutions of increasing concentration in the RTIL.

For an initial concentration, C_0, higher than the intrinsic solubility of the $AgCl_{(s)}$ species, S_0 ($C_0 > S_0$), the distinctive condition of a heterogeneous system is met, allowing the determination of the solubility product constant, K_{sp}, of the $AgCl_{(s)}/Ag^+$ pair through a Gunnar-Gran type adjustment using the added volume data and the cell potential obtained before the equivalence point (Fig. S4, Appendix C, Supporting Information) [30]. A white precipitate was observed during the titration, whose abundance visually increased from the beginning of the process until the equivalence point, remaining constant thereafter. Potentiometric titration continued up to a 400% excess of titrant relative to the first equivalence volume to form the $[AgCl_2]^-$ and $[AgCl_3]^{2-}$ species, for which there is evidence in these solvents and to estimate the values of the global formation constants, β_2 and β_3, respectively (Fig. S6, Appendix C, Supporting Information). The final titration phase corresponds to a plateau in the cell potential values determined by the $Ag^{+/0}$ redox pair.

The second scenario was examined under one condition: the initial concentration was below the intrinsic solubility, $C_0 < S_0$. Under this premise, a homogeneous system was established, so the titration of $[C_2mim]Cl$ in the RTIL with additions of $Ag[NTf_2]$ resulted in the formation of the soluble [AgCl] species. No solids were observed during the analytical process (Fig. S5, Appendix C, Supporting Information). The cell potential data obtained before the equivalence point were fitted to a Gunnar-Gran function to estimate the global formation constant, β_1, of the soluble [AgCl] species, using the law of mass action for the $[AgCl]/Ag^+$ pair. The final titration stage showed a potential plateau determined by the same process as in the previous scenario.

The values of the constants obtained from the previous Gunnar-Gran type adjustments provided a reference point for applying the ulterior non-linear adjustments, according to Brown's methodology [31]. The Method of Extended Ringbom's Coefficients (MERC) [32], commonly used in aqueous media to describe equilibrium systems, was successfully adapted to this ionic liquid to get a fourth-degree polynomial describing the theoretical titration curve based on electroneutrality balance during the potentiometric titration, incorporating condensed species for a more accurate description of the systems. Once the polynomial was established, the Solver® tool, available as an add-in in Microsoft Excel®, was used to adjust the theoretical values of pAg or pCl (calculated from the recorded cell potential values), minimizing the sum of squared differences with respect to the volume. The goodness of the non-linear fit was verified in terms of $R^{2,}$ showing that theoretical titration curves closely matched the experimental data (Fig. 2**(A)** and 2**(B)**). The logarithm of the formation constants set was reported with a 95.45% confidence interval corresponding to a coverage factor, k = 2 (Table 2), assuming normally distributed data.

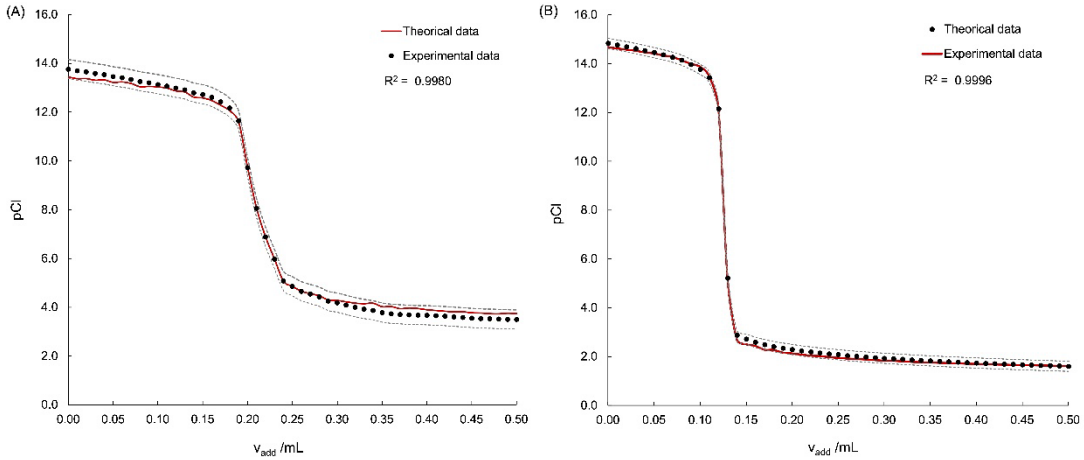

Fig. 2. Experimental curves, represented by a solid red line, and non-linear fits, represented by dots for **(A)** Records of OCP evolution of a Ag^0 indicator electrode during the titration of $[C_2mim]Cl$ ($C_0 = 0.10001$ mol L^{-1}) with additions of $Ag[NTf_2]$ ($C_{Ag^+} = 0.09972$ mol L^{-1}) in $[C_4mim][NTf_2]$; and **(B)** records of OCP evolution of a $Ag^0|AgCl_{(s)}$ indicator electrode during the titration of $Ag[NTf_2]$ ($C_0 = 0.09972$ mol L^{-1}) with additions of $[C_2mim]Cl$ ($C_{Cl^-} = 0.10001$ mol L^{-1}) in $[C_4mim][NTf_2]$. Additionally, the confidence intervals are outlined with a dashed line.

J. Mex. Chem. Soc. **2025**, *69*(4)
Regular Issue

ISSN-e 2594-0317

A similar experiment was conducted in an aqueous solution, where aliquots of NaCl were added to a solution of $AgNO_3$. A typical potential response was obtained (results not shown), with an initial constant potential region given by the $AgCl_{(s)}/Ag^+$ pair and a second plateau determined by the $AgCl_{(s)}/Cl^-$ redox pair (Fig. S7, Appendix C, Supporting Information). The methodology described above was successfully applied to this system, yielding a pK_{sp} value of 9.4 ± 0.5 for the $AgCl_{(s)}/Ag^+$ pair [33,34].

Table S5, Appendix E, Supporting Information, presents the set of polynomials that describe the different theoretical titration curves carried out both in $[C_4mim][NTf_2]$ and in aqueous media, the Gunnar-Gran equations and the explicit expressions of the distributive molar fractions, φ_i, used in such polynomials.

On the other hand, the residual analysis of silver(I) in the aqueous phase of each extraction assay was performed through potentiometric titration using NaCl 0.1 mol L^{-1} as the titrant. The experimental titration curve shows a typical profile of a quantitative reaction. At the beginning of the titration, the solution is colorless; with the first addition of the titrant, turbidity appears due to the formation of a white solid, which corresponds to the formation of $AgCl_{(s)}$. Subsequently, the formation of a violet solid was observed until the equivalence point. Once the endpoint of the titration was exceeded, the precipitate was partially dissolved. The determination of the endpoint for the quantification of silver content in the aqueous phase was carried out using the first derivative, $\Delta pCl/\Delta V$ *vs*. V_{added}. Table S3, Appendix C, Supporting Information presents the amount of substance (in terms of Ag found) in the aqueous phase.

Total determination of soluble silver(I) in $[C_4mim][NTf_2]$

The total solubility of silver(I) in the RTIL, denoted as S_{max}, is given by contributions from molecular and ionic solubility as described by Equation 1.

$$S_{max} = \sum_{n=0}^{i} [[AgCl_n]^{1-n}] = [Ag^+] + [[AgCl]] + [[AgCl_2]^-] + [[AgCl_3]^{2-}] + \cdots \qquad \text{Equation 1}$$

To determine the maximum solubility of Ag(I) in $[C_4mim][NTf_2]$ and its concentration in such phase, several anodic stripping square wave voltammetry (ASSWV) assays were conducted on a glassy carbon electrode using a coordinating medium in aqueous solution [35]. The standard addition method was employed on an aliquot of the sample, followed by the addition of a standardized $AgNO_3$ solution (Fig. S8, Appendix C, Supporting Information). The maximum solubility of Ag(I) in $[C_4mim][NTf_2]$ was determined to be $\log (S_{max}/M) = (2.8 \pm 0.5)$. This solubility value is consistent with reports on other imidazolium-based ionic solvents, where the hydrocarbon chain at position number one of the imidazole ring notably influences the value of S_0. Increasing the number of carbon atoms in the chain leads to a decrease in S_0 [15]. The amount of substance in the nonaqueous phase was determined successfully, and it was observed that its value depends on the volume ratio, $p(V_{org}/V_{ac})$; these results are shown in Table S3, Appendix C, Supporting Information.

Estimation of the conditional extraction constant

The equilibrium associated with the extraction of Ag^+ in the H_2O–$[C_4mim][NTf_2]$ system is represented in Equation 2, where the species in the nonaqueous solvent is denoted with a straight line over the condensed formula as follows $\overline{Ag^+}$; while the species in the aqueous medium simply as Ag^+ [36,37].

$$\overline{Ag^+} \rightleftarrows Ag^+ \qquad \text{Equation 2}$$

However, in the aqueous phase, both soluble and insoluble species may form due to the interaction of silver(I) with the solvent, depending on the pH values in such phase [38]. The reaction scheme considering these reactions is outlined in Equation 3.

$$\overline{Ag^+} \quad \rightleftarrows \quad \begin{array}{c} AgO_{0.5\,(s)} \\ \downarrow\uparrow \\ Ag^+ \\ \downarrow\uparrow \\ [Ag(OH)_n]^{1-n} \end{array} \qquad \text{Equation 3}$$

J. Mex. Chem. Soc. **2025**, *69*(4)
Regular Issue

ISSN-e 2594-0317

A conditional extraction constant is defined since the chemical species Ag^+ in the aqueous medium significantly depends on the system's pH. According to the law of mass action, this constant is defined as the ratio between the total concentration of Ag^+ in the nonaqueous phase and the total concentration of Ag^+ in the aqueous phase [39], as represented in Equation 4.

$$K'_E = \frac{[\overline{Ag^+}]}{[Ag^+]'} = \frac{[\overline{Ag^+}]}{[Ag^+]\bar{\alpha}_{Ag^+(H)}} \qquad \text{Equation 4}$$

By multiplying this conditional extraction constant by the alpha speciation coefficient in the heterogeneous medium, defined according to the Method of Extended Ringbom's Coefficient under the working conditions [32], $\alpha_{Ag^+(H)}$, the apparent extraction constant can be determined, as shown in Equation 5.

$$K_E = K'_E\, \alpha_{Ag^+(H)} = \frac{[\overline{Ag^+}]}{[Ag^+]} \qquad \text{Equation 5}$$

In each system, the amount of Ag^+ in both phases was quantified, and based on the volume ratio, the values of the conditional and apparent extraction constants were calculated under buffered aqueous conditions. The results of this determination are presented in Table 1.

Table 1. Conditional extraction constant values, K_E', apparent extraction constant, K_E, at different pH values and volume ratios, $p(V_{org}/V_{aq})$.

System	$P(V_{org}/V_{aq})$	pH	K_E'	K_E	log K_E
A	-0.01	3.47	362.4	362.5	2.56
B	-0.22	3.47	217.0	217.0	2.34
C	0.17	3.47	186.0	186.0	2.27
D	0.20	3.47	91.8	91.8	1.96
E	0.20	7.86	78.1	128.7	2.11
F	0.19	11.49	72.8	175.7	2.24
G	0.70	8.64	34.9	627.6	2.78

Thus, the apparent extraction constant, expressed in logarithm terms, for silver(I) in the water-1-butyl-3-methylimidazolium bis(trifluorosulfonyl imide) system is log (K_E) = 2.32 ± 0.27.

Compilation of estimated equilibrium constants for Ag^+–Cl^-–e^- redox system in [C_4mim][NTf_2]

Table 2 summarizes the calculated parameters pertaining to the Ag^+–Cl^-–e^- system in [C_4mim][NTf_2]. Fig. 3 presents the solubility diagram for these systems, constructed by deducing a nonsegmented polynomial considering phase transition and incorporating an extended concept of Ringbom's side reaction coefficients (Method of Extended Ringbom's Coefficients) that is usually applied to describe chemical speciation in multicomponent systems (Appendix E, Supporting Information) [15,32]. Although there is evidence of the formation of ion pairs or other associated ionic species in RTILs [40], the effective concentration, being relatively high, often surpasses the concentration of the solutes dissolved in them. Consequently, the ionic strength in these systems is determined mainly by ions originating from the solvent itself. This phenomenon establishes the baseline for estimated equilibrium constants, making them apparent constants. Similarly, the estimated potentials are formal redox potentials, denoted as E°' [41–43].

J. Mex. Chem. Soc. **2025**, *69*(4)
Regular Issue

ISSN-e 2594-0317

Table 2. Mean formal potential and apparent values of thermodynamic parameters obtained by potentiometry and voltammetry measurements carried out in $[C_4mim][NTf_2]$ (N = 5).

Parameter	Couple (donor/receiver)	Value
$E°'/V^a$	Ag^0/Ag^+	1.604 ± 0.006
$E°'/V^a$	$Ag^0/[AgCl_3]^{2-}$	0.339 ± 0.007
pK_{sp}	$AgCl_{(s)}/Ag^+$	16.6 ± 0.1
pK_{sp}^b	$AgCl_{(s)}/Ag^+$	9.4 ± 0.5
log (β_1)	$[AgCl]/Ag^+$	13.1 ± 0.1
log (β_2)	$[AgCl_2]^-/Ag^+$	16.6 ± 1.5
log (β_3)	$[AgCl_3]^{2-}/Ag^+$	17.9 ± 1.7
log (S_{max})	$AgCl_{(s)}/[AgCl]$	-2.8 ± 0.5
log (K_E)	$(Ag^+)_{RTIL}/(Ag^+)_{H_2O}$	2.3 ± 0.3
C_{H_2O} /ppm	-	121.3 ± 3.4

[a]The potential values are presented relative to the $[Co(Cp)_2]^{+/0}$ redox couple.
[b]Determined in aqueous media.

With the constant values estimated in this work, it was possible to construct the Predominance States Diagram (PSD) of the logarithm of the conditional extraction constant as a function of pCl (Fig. 3) for the $[C_4mim][NTf_2]$-water interface. The diagram was constructed using Equation S6, presented in Appendix E, Supporting Information. It is imperative to highlight that in the present diagram, pCl is evaluated equally in both phases.

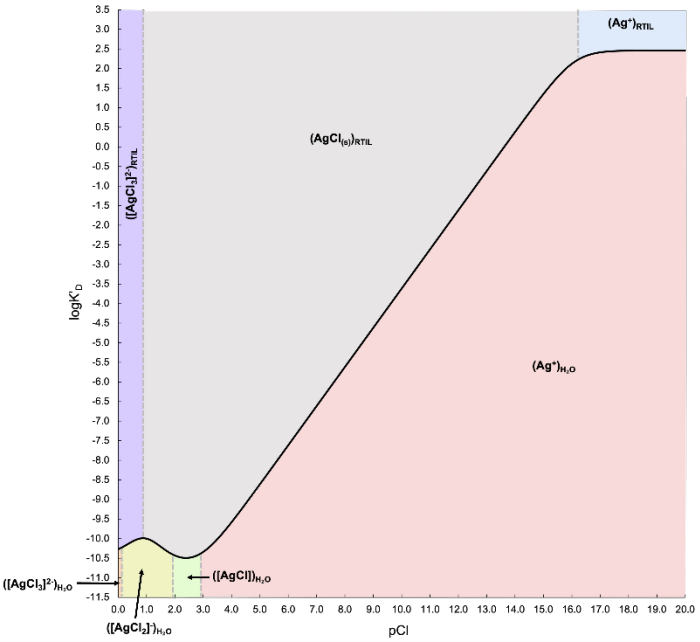

Fig. 3. Predominance Diagram of States of the logarithm of the conditional extraction constant as a function of pCl at $p(V_{org}/V_{aq})$ = -0.01 and an initial concentration of Ag(I)' in $[C_4mim][NTf_2]$ of 0.3 M.

J. Mex. Chem. Soc. **2025**, *69*(4)
Regular Issue

ISSN-e 2594-0317

This diagram can be interpreted as analogous to traditional complex formation diagrams, wherein the reactants are positioned at the apex of the diagram while the products occupy the lower region. Also, it allows us to discern how variations in the pCl value, evaluated at the same concentration in both phases, influence the direction of extraction, thereby facilitating the understanding of why trace water contamination does not affect these systems, provided that pCl values remain low. The subsequent section dedicated to constructing true reference electrodes offers a more detailed explanation.

Evaluation of the reference electrodes constructed in $[C_4mim][NTf_2]$

To evaluate the stability of the electrode potential values over time and determine the pCl and pAg' at which the electrode potential drift of the reference electrodes is minimal, the $E_{½}$ of the $[Co(Cp)_2]^{+/0}$ redox couple was determined by CV using these reference electrodes (Appendix F, Supporting Information) in $[C_4mim][NTf_2]$. The drift was assessed for four electrodes constructed under the conditions described in Appendix A of the Supporting Information over a period of 3500 h, as shown in Fig. 4.

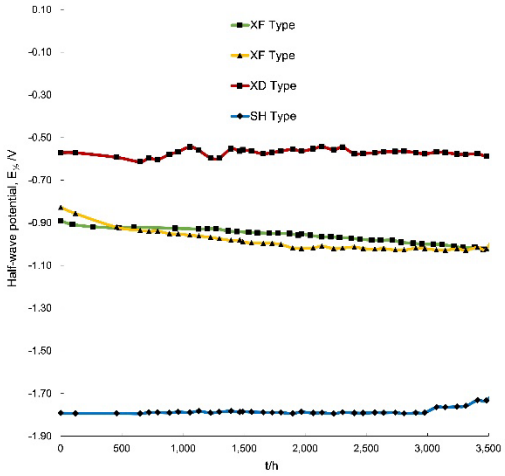

Fig. 4. Variation of the electrode potential for the constructed reference electrodes over time using filling solutions of $[C_2mim]Cl$ and $Ag[NTf_2]$ with concentrations of C = 0.0100 mol L^{-1} (Type XF); C = 1.000 mol L^{-1} (Type XD) and C = 0.3000 mol L^{-1} (Type SH) in $[C_4mim][NTf_2]$. The $E_{1/2}$ value obtained by CV for the $[Co(Cp)_2]^{+/0}$ redox couple is reported.

The electrode potential values obtained were practically constant from the early days of fabrication, with variations not exceeding ±10 mV. The potential drift observed for the reference electrodes over time may be attributed to the gradual degradation of the $AgCl_{(s)}$ coating due to UV radiation, causing the photoreduction of the Ag^0 coating [44]. This phenomenon was not observed in REs that were permanently stored inside the Bel-Art desiccator due to the device's UV protection. Although water absorption was observed by the RTIL that make up the REs when stored without protection from atmospheric humidity, these devices can recover their initial potential value after drying for 24 h in an oven at 90 °C.

It was observed that Type XD and SH electrodes showed the lowest potential drifts, 0.53 μV h^{-1} and 0.58 μV h^{-1}, respectively, compared to Type XF electrodes, which had a drift of approximately 9.5 μV h^{-1}. Thus, according to the solubility diagram in Fig. 5, constructed by deducing a nonsegmented polynomial considering phase transition and incorporating the MERC, the Type D electrode contains buffering conditions to maintain the speciation of Ag(I) predominantly in the form of $[AgCl_3]^{2-}$. On the other hand, the Ag^0/Ag^+ redox couple proves to be a system with a rapid and stable response in this ionic solvent. Although it has been reported that for nonaqueous systems, the most common RE is the Ag^0/Ag^+, and in this work, it has been shown that its potential drift is very low, it should be considered that the extraction of this cation is possible when the $[C_4mim][NTf_2]$ comes into contact with water, causing a perceptible change in its concentration in the nonaqueous phase and consequently, a more significant potential drift. Thus, the REs based on the concomitant

J. Mex. Chem. Soc. **2025**, *69*(4)
Regular Issue

ISSN-e 2594-0317

$Ag^0|AgCl_{(s)}$ interface offer a better response to humidity conditions even to high pCl values in the nonaqueous phase, since the extraction of the $[AgCl_n]^{1-n}$ species from the $[C_4mim][NTf_2]$ towards water is not favored.

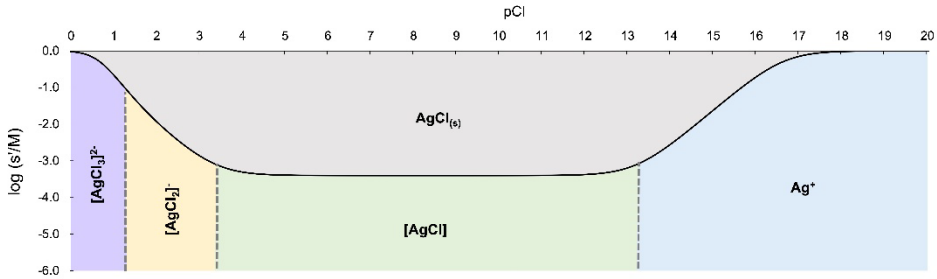

Fig. 5. Solubility diagram of $AgCl_{(s)}$ in $[C_4mim][NTf_2]$. Depicted in blue for Ag^+; green for [AgCl]; yellow for $[AgCl_2]^-$; purple for $[AgCl_3]^{2-}$; and red for $AgCl_{(s)}$.

The liquid junction potential was calculated using the Henderson equation [45] based on the limiting molar conductivity values of the corresponding chemical species [46]. This calculation resulted in potential values below the resolution limit of the instruments used in this study. Additionally, Bülhmann *et al.* have reported that liquid junction potentials in reference electrodes equipped with porous liquid junctions, such as Vycor® type, tend to decrease as ionic strength increases. Since ions are the primary constituents of RTILs, the ionic strength in these solvents is significantly high, resulting in remarkably low liquid junction potential values [47].

Additionally, the water content in this ionic liquid was quantified through electrochemical techniques [48], yielding an approximate water content of 121.3 ppm after a drying process of 48 h in an oven at 90 °C. If, in Equation S6, the concentration of Cl^- in the inner chamber of the Type DB electrode is evaluated under a hypothetical condition of high relative humidity, where a significant amount of water might infiltrate the ionic liquid, a log K_E' value of -15.5 would be obtained. This value indicates that the equilibrium of Ag(I) in the RTIL at elevated pCl values, in $[C_4mim][NTf_2]$ phase, does not favor extraction into the aqueous phase, thus ensuring a homogeneous and unaltered coating on the reference electrode, even in the presence of water contamination.

A similar study was carried out in parallel using commercial reference electrodes for use in aqueous solution, finding that those based on the $Ag^0|AgCl_{(s)}$ interface presented average potential drifts of 7.18 $\mu V\ h^{-1}$ in the same period when using a solution of ferrocenemethanol ($[Fe(Cp)_2CH_2OH)]$), $C \approx 25$ mmol L^{-1} in the presence of $LiClO_4$, C = 0.1 mol L^{-1}, as a redox reference system (Appendix G, Supporting Information).

Conclusions

In this work, we present a methodology to describe the chemical speciation of the system $[AgCl_n]^{1-n}/Ag^0$ in both $[C_4mim][NTf_2]$ and aqueous solution, using various electrochemical techniques to obtain formal potential values and apparent constants associated with the concurrent chemical equilibria in this ionic liquid. Additionally, the logarithm of the extraction constant of Ag^+ in the water–RTIL interface was reported as log $K_E = (2.3 \pm 0.3)$, indicating that the extraction of silver from the 1-butyl-3-methyl imidazolium bis(trifluorosulfonyl imide) ionic liquid with water is favored, particularly at high pCl values imposed in both phases. This phenomenon suggests potential applications for purifying this ionic liquid using water, a ubiquitous and low-cost solvent.

The information collected is useful for describing the processes responsible for the potential observed in the true Type I and Type II reference electrodes, constructed based on the concomitant $Ag^0|[AgCl_n]^{1-n}$ interface, for use in this ionic solvent. For the RTIL $[C_4mim][NTf2]$, it was found that the best electrode configuration was $Ag^0|AgCl_{(s)}||[C_2mim]Cl$, 1.000 mol L^{-1}, $[C_4mim][NTf_2]||$ (0.53 $\mu V\ h^{-1}$), which is competitive with reference electrodes reported in aqueous media. In this way, the reference electrodes presented in this work appear robust and have reproducible potential values. Also, it has been determined that under the pCl values buffered for each phase in the configuration of the RE (low ones in the RTIL and high ones in the aqueous

J. Mex. Chem. Soc. **2025**, *69*(4)
Regular Issue

ISSN-e 2594-0317

medium), the silver(I) does not transfer to the aqueous phase, thereby maintaining a homogeneous coating inside de REs without causing any alteration in their composition.

In summary, the description of chemical reactivity based on the Method of Extended Ringbom's Coefficients was applicable in ionic liquids and offers an opportunity to optimize the design of reference electrodes and specific reaction media, applying what we described in new RTILs.

Acknowledgments

This work was supported by UNAM-PAPIIT IA202122 and UNAM-PAPIIT IA207724. J. Ruvalcaba-Juárez is thankful for the scholarship provided by CONAHCyT (No. 1099976).

References

1. Lei, Z.; Chen, B.; Koo, Y.-M.; MacFarlane, D. R. *Chem. Rev.* **2017**, *117*, 6633–6635. DOI: https://doi.org/10.1021/acs.chemrev.7b00246.
2. Wasserscheid, P.; Welton, T., in: *Ionic Liquids in Synthesis*, 2nd ed.; Wiley, **2008**; Vol. 1. DOI: 10.1002/9783527621194.
3. Barrosse-Antle, L. E.; Bond, A. M.; Compton, R. G.; O'Mahony, A. M.; Rogers, E. I.; Silvester, D. S. *Chem. Asian J.* **2010**, *5*, 202–230. DOI: https://doi.org/10.1002/asia.200900191.
4. Caminiti, R.; Gontrani, L., in: *The Structure of Ionic Liquids*, 1st ed.; Springer, **2013**. DOI: https://doi.org/10.1007/978-3-319-01698-6.
5. Tiago, G. A. O.; Matias, I. A. S.; Ribeiro, A. P. C.; Martins, L. M. D. R. S. *Molecules.* **2020**, *25*, 5812. DOI: https://doi.org/10.3390/molecules25245812.
6. Cruz, C.; Ciach, A. *Molecules.* **2021**, *26*, 3668. DOI: https://doi.org/10.3390/molecules26123668.
7. Piatti, E.; Guglielmero, L.; Tofani, G.; Mezzetta, A.; Guazzelli, L.; D'Andrea, F.; Roddaro, S.; Pomelli, C. S. *J. Mol. Liq.* **2022**, *364*, 120001. DOI: https://doi.org/10.1016/j.molliq.2022.120001.
8. Ratti, R. *Adv. Chem.* **2014**, 1–16. DOI: https://doi.org/10.1155/2014/729842.
9. Riaño, S. Ionic Liquids as Green Solvents: A Critical Analysis, in: *Encyclopedia of Green Chemistry*; Elsevier, **2025**; 43–53. DOI: https://doi.org/10.1016/b978-0-443-15742-4.00019-3.
10. Gong, K.; Fang, Q.; Gu, S.; Li, S. F. Y.; Yan, Y. *Energy Environ. Sci.* **2015**, *8*, 3515–3530. DOI: https://doi.org/10.1039/c5ee02341f.
11. Torriero, A. A. J., in: *Electrochemistry in Ionic Liquids. Volume 1: Fundamentals*; Springer, **2015**; Vol. 1. DOI: https://doi.org/10.1007/978-3-319-13485-7.
12. Snook, G. A.; Best, A. S.; Pandolfo, A. G.; Hollenkamp, A. F. *Electrochem. commun.* **2006**, *8*, 1405–1411. DOI: https://doi.org/10.1016/j.elecom.2006.07.004.
13. Huber, B.; Roling, B. *Electrochim. Acta.* **2011**, *56*, 6569–6572. DOI: https://doi.org/10.1016/j.electacta.2011.02.055.
14. Horwood, C.; Stadermann, M. *Electrochem. Commun.* **2018**, *88*, 105–108. DOI: https://doi.org/10.1016/j.elecom.2018.02.005.
15. García-Mendoza, A.; Aguilar-Cordero, J. C. *Electrochim. Acta.* **2019**, *302*, 344–351. DOI: https://doi.org/10.1016/j.electacta.2019.02.029.
16. Nevell, T. G.; Walsh, F. C. *Trans. IMF* **1992**, *70*, 144–147. DOI: https://doi.org/10.1080/00202967.1992.11870962.
17. Inzelt, G.; Lewenstam, A.; Scholz, F., in: *Handbook of Reference Electrodes*; Springer, **2013**. DOI: https://doi.org/10.1007/978-3-642-36188-3_6.
18. Bard, A. J.; Faulkner, L. R.; White, H. S. *Electrochemical Methods - Fundamentals and Applications*, 3rd ed.; Wiley, **2022**. DOI: https://doi.org/10.1007/s11243-023-00555-6.

J. Mex. Chem. Soc. **2025**, *69*(4)
Regular Issue

ISSN-e 2594-0317

19. Bard, A. J., Inzelt, G., Scholz, F., in: *Electrochemical Dictionary*; Springer, **2008**. DOI: https://doi.org/10.1007/978-3-540-74598-3.
20. Sukardi, S. K.; Zhang, J.; Burgar, I.; Horne, M. D.; Hollenkamp, A. F.; MacFarlane, D. R.; Bond, A. M. *Electrochem. commun.* **2008**, *10*, 250–254. DOI: https://doi.org/10.1016/j.elecom.2007.11.022.
21. Scholz, F., in: *Electroanalytical Methods, Guide to Experiments and Applications*; Springer, **2010**. DOI: https://doi.org/10.1007/978-3-642-02915-8.
22. Inzelt, G.; Lewenstam, A.; Scholz, F., in: *Handbook of Reference Electrodes*; Springer, **2013**. DOI: https://doi.org/10.1007/978-3-642-36188-3_6.
23. Lockett, V.; Horne, M.; Sedev, R.; Rodopoulos, T.; Ralston, J. *Phys. Chem. Chem. Phys.* **2010**, *12* , 12499–12512. DOI: https://doi.org/10.1039/c0cp00170h.
24. Fedorov, M. V.; Kornyshev, A. A.; Georgi, N. *Electrochem. commun.* **2010**, *12*, 296–299. DOI: https://doi.org/10.1016/j.elecom.2009.12.019.
25. Yalcinkaya, F.; Powner, E. T. *Méd. Eng. Phys.* **1997**, *19*, 299–301. DOI: https://doi.org/10.1016/s1350-4533(96)00034-3.
26. Fleischmann, M.; Hiddleston, J. N. *J. Phys. E: Sci. Instrum.* **2002**, *1*, 667. DOI: https://doi.org/10.1088/0022-3735/1/6/424.
27. Martell, A. E.; Smith, R. M., in: *Critical Stability Constants. Volume 4: Inorganic Complexes*; Springer, **1976**; Vol. 4. DOI: https://doi.org/10.1007/978-1-4757-5506-0.
28. Rodil, E.; Aldous, L.; Hardacre, C.; Lagunas, M. C. *Nanotechnology* **2008**, *19*, 105603–105608. DOI: https://doi.org/10.1088/0957-4484/19/10/105603.
29. Martell, A. E.; Smith, R. M., in: *Critical Stability Constants. Volume 6: Second Supplement*; Springer, **1989**; Vol. 6. DOI: https://doi.org/10.1007/978-1-4615-6764-6.
30. Gran, G. *Acta Chem. Scand.* **1950**, *4*, 559–577. DOI: https://doi.org/10.3891/acta.chem.scand.04-0559
31. Brown, A. M. *Comput. Methods Programs Biomed.* **2001**, *65*, 191–200. DOI: https://doi.org/10.1016/S0169-2607(00)00124-3.
32. Briones-Guerash-S. U.; García-Mendoza, A.; Aguilar-Cordero, J. C. *J. Chem. Educ.* **2023**, *100*, 4663–4673. DOI: https://doi.org/10.1021/acs.jchemed.3c00790.
33. Davies, C. W.; Jones, A. L. *Discuss. Faraday Soc.* **1949**, *5*, 103–111. DOI: https://doi.org/10.1039/df9490500103.
34. Kim, J. I.; Duschner, H. *J. Inorg. Nucl. Chem.* **1977**, *39*, 4771–4478.
35. Dilleen, J. W.; Sprules, S. D.; Birch, B. J.; Haggett, B. G. D. *The Analyst* **1998**, *123*, 2905–2907. DOI: https://doi.org/10.1039/a806344c.
36. Johansson, P.-A.; Karlberg, B.; Thelander, S. *Anal. Chim. Acta* **1980**, *114*, 215–226. DOI: https://doi.org/10.1016/s0003-2670(01)84293-8.
37. Gavazov, K. B. *Acta Chim. Slov.* **2012**, *59*, 1–17.
38. Fritz, J. J. *J. Solut. Chem.* **1985**, *14*, 865–879. DOI: https://doi.org/10.1007/bf00646296.
39. Lloyd, P. J. D., in: *Solvent Extraction Principles and Practice, Revised and Expanded*, 2nd ed.; Marcel Dekker, **2004**. DOI: https://doi.org/10.1201/9780203021460-14.
40. Ma, L.; Zhong, Z.; Hu, J.; Qing, L.; Jiang, J. *J. Phys. Chem. B* **2023**, *127*, 5308–5316. DOI: https://doi.org/10.1021/acs.jpcb.3c01559.
41. Tokuda, H.; Tsuzuki, S.; Susan, M. A. B. H.; Hayamizu, K.; Watanabe, M. *J. Phys. Chem. B* **2006**, *110*, 19593–19600. DOI: https://doi.org/10.1021/jp064159v.
42. Gebbie, M. A.; Smith, A. M.; Dobbs, H. A.; Lee, A. A.; Warr, G. G.; Banquy, X.; Valtiner, M.; Rutland, M. W.; Israelachvili, J. N.; Perkin, S.; Atkin, R. *Chem. Commun.* **2016**, *53*, 1214–1224. DOI: https://doi.org/10.1039/c6cc08820a.
43. Nordness, O.; Brennecke, J. F. *Chem. Rev.* **2020**, *120*, 12873–12902. DOI: https://doi.org/10.1021/acs.chemrev.0c00373.
44. Yalcinkaya, F.; Powner, E. T. *Med. Eng. Phys.* **1997**, *19*, 299–301. DOI: https://doi.org/10.1016/s1350-4533(96)00034-3.

J. Mex. Chem. Soc. **2025**, *69*(4)
Regular Issue

ISSN-e 2594-0317

45. Mousavi, M. P. S.; Saba, S. A.; Anderson, E. L.; Hillmyer, M. A.; Bühlmann, P. *Anal. Chem.* **2016**, *88* (17), 8706–8713. DOI: https://doi.org/10.1021/acs.analchem.6b02025.
46. Vranes, M.; Dozic, S.; Djeric, V.; Gadzuric, S. *J. Chem. Eng. Data* **2012**, *57*, 1072–1077. DOI: https://doi.org/10.1021/je2010837.
47. Zoski, C. G., in: *Handbook of Electrochemistry*; Oxford, **2006**.
48. García-Mendoza, A.; Aguilar, J. C. *Electrochim. Acta*. **2015**, *182*, 238–246. DOI: https://doi.org/10.1016/j.electacta.2015.09.045.